MACIEJ KRASIŃSKI [*], *ANDRZEJ TROJNACKI* [*]

EXPERIMENTAL INVESTIGATIONS OF METAL HIGH-PRESSURE "2-DELTA" GASKET

The paper deals with experimental investigations of a set of metal "2-delta" gaskets of different depth. The gaskets were examined under assembly conditions, i.e. placed in their seats and loaded with the compressive assembly force with no operating pressure applied to the closure. The electric resistance wire strain gauges were used to measure the circumferential and axial strains at the inner cylindrical surface of the gaskets. The plastic deformations of the contact surface of the seats were measured after disassembly of the closures. The material tests were carried out to determine real mechanical properties of materials applied for the gaskets and the seats. The results of experiment were compared with the analytical approach. The plastic deformations were taken into account in the analytical solution of the contact region between the gasket and the seats. The results of experiment and analytical approach were verified by FEM calculations, which take into account linear hardening of the material, friction and contact effects.

1. Introduction

Technical requirements of modern power engineering systems and advanced chemical technologies (pressure, temperature), application of corrosion-resistant materials (high quality alloy steels) and further brief foredesigns (e.g. possibility of convenient uncoupling of the gasketed members) cause serious difficulties with leak tightness of high-pressure equipment. In such cases, the metal gaskets are often used to seal the heads of pressure vessels and temporary pipe connections. These gaskets provide a satisfactory static seal and additionally are rust-proof, chemical resistant and stable to heat. Simple flange joints with sheet metal gaskets are used in closures operating at relatively low pressure, less than 32 MPa. Their dimensions are up to stan-

---

[*] *Institute of Machine Design, Cracow University of Technology, Al. Jana Pawła II No. 37, 31-864 Kraków, Poland; E-mail: mkr@mech.pk.edu.pl; atroj@mech.pk.edu.pl*

dard as well as design (selection) procedures, which for typical applications is regulated by the Office of Technical Inspection (OTI) code or appropriate standards (e.g. EN or ASME).

For higher-pressure applications (100 MPa or more), another sealing systems with metal gaskets are used [2, 3, 10]. Many modifications of such sealing systems exist with linear or face contact between the members of the sealing. Some closures are known as self-sealing closures, because they tend to tighten with increasing internal pressure. One of them is the closure with "2-delta" gasket, developed directly from the flat compression gasket at about the time high-pressure processes came into industrial use. This gasket is better adapted to small rather than to large openings and is suitable to seal additional accessories.

The closures with "2-delta" gaskets are not regulated by standards, so in each individual case of technical application a set of complex and time-consuming calculations of strength and of leak tightness must be carried out. The assembly conditions and technical inspection requirements must be determined. The materials for each member of the joint and their technology must be specified as well.

The paper follows earlier theoretical investigations of the authors devoted to verification of several analytical models of the "2-delta" gasket by FEM modeling [7] and to the numerical analysis of leak tightness of the closure [8]. The aim of the paper is the experimental verification of a certain numerical computational model of "2-delta" gasket, which could be applied in engineering calculations of geometry, material properties, assembly requirements and operating parameters of the closures.

2. Engineering example and the principle of the gasket

The "2-delta" gasket is a certain type of self-sealing gaskets for very high-pressure power and chemical equipment. It is used to seal small openings appropriate for casings of pressure gauges, connections of gas inlets, catalyst feeders or housings of thermocouples and reactor electrodes. Engineering example of the joint is shown in Fig. 1. The closure is successfully applied [16] in the heavy-duty chemical installation operating at the pressure 200 MPa, and is used to seal the housing of the electrode. The metal gasket 1 is placed with a certain diameter clearance into the seat of the reactor vessel 2 and pressed with the screw joint 4. The screw joint produces an initial contact pressure between the working surfaces of the gasket and of the seat and the screw joint. A seal is formed between the sides of the gasket and the seat of each mating member.
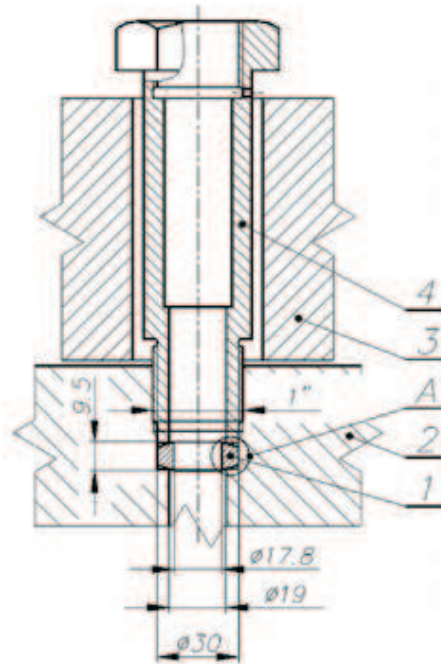
Fig. 1. Engineering example of the closure with the "2-delta" gasket: 1 – metal "2-delta" gasket,
2 – reactor vessel, 3 – clamping ring, 4 – screw joint

The working sealing surfaces of the gasket must be of high hardness. The gaskets are usually made of special alloy toughening steel (e.g. 36CrN-iMo4 – EN 10250-3:1999) with yield point of 900 MPa, tensile strength of 1100÷1300 MPa, which are hardened to 55 HRC. The mating members (the seats) are made of alloy hot-work steel (e.g. 32CrMo12 – EN 10250-3:1999), with yield point of 680 MPa, tensile strength of 900 MPa, and of ultimate elongation greater than 12%.

The hardened sealing surfaces of the gasket are sloped to the surface perpendicular to the axis of the closure with a certain angle α (Fig. 2). When assembling a closure, a sufficient force F must be applied in order to ensure that both relatively softer segments of the sharp-edged seat deform at the width e, and initial pressure q is obtained there. Internal pressure p acting on the members of the closure generates a decrease in the assembly force F and a relevant decrease in initial pressure q. On the other hand, as the pressure p is applied, the gasket expands because its stiffness is much lower than that of the seats, and an appropriate assembly clearance makes radial displacements of the outer surface possible. The assembly clearance is selected individually to each joint and for the exemplary gasket shown in Fig. 1 it was fixed between 0.076 mm and 0.177 mm. The principle of the
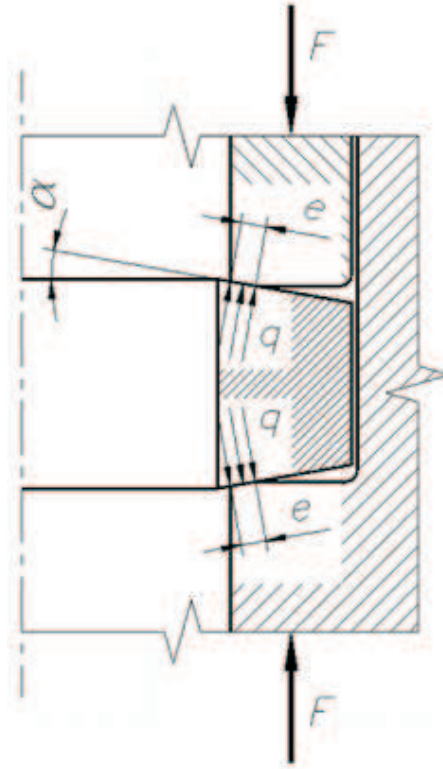
Fig. 2. Distribution of initial contact pressure under the assembly force in the closure with the "2-delta" gasket (detail A in Fig. 1)

gasket is that, after an initial seal has been made, internal pressure pushes thick inside periphery of the gasket, forcing a tighter seal to be made on the sealing surface located along the thinner portion of the gasket. Thus, the unsupported-area principle comes into effect. Because of their specific features, the considered closures with "2-delta" gasket are used in heavy-duty equipment operating at very high pressures of the order of hundreds MPa.

The "2-delta" gaskets give satisfactory service where a closure does need not to be opened frequently. In the opposite case, they are somewhat imprac-tical. Hardened gasket may by used several times, but relatively softer seats suffer from plastic deformation, and need regeneration before repeated assem-bly. The advantage of the closure with "2-delta" gasket is that its elements are not too complex and don't need high dimensional accuracy. Special attention must be paid, however, to the working conical sealing surfaces which must be of high surface finish.

3. The test stand and program of experiment

The test stand was designed to examine the gaskets under assembly loading only, with no operating pressure applied. The construction of the test stand is shown in Fig. 3. The examined "2-delta" gasket 3 is located in the holder 2, which positions the gasket with respect to the seats 4. The contact pressure at the sealing surfaces of the gasket providing the leak tightness of the closure is produced by the loading applied to the stripper punch 1 guided in the holder.
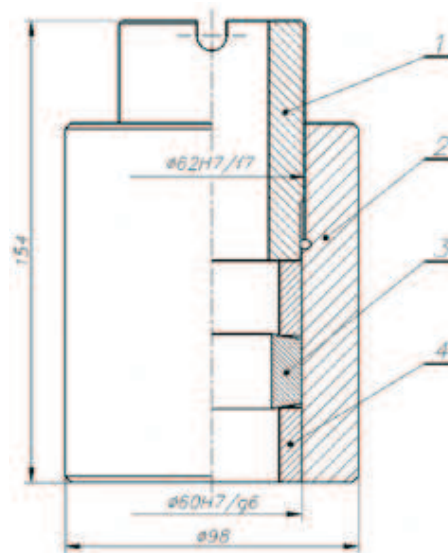

Fig. 3. Test stand: 1 – stripper punch, 2 – holder, 3 – "2-delta" gasket, 4 – seats

The gaskets were made of the forged bar of 40H2MF steel and the seats of 45HN steel using machining, and were subjected to the heat treatment. Both materials belong to the constructional steels suitable for toughening and hardening (PN-89/H-84030/04), and have no equivalents in EN 10027-1, 2:1994. An ultrasonic method was applied to test the quality (the cracks) of the semi-finished steel. Four sets of gaskets and the corresponding sectional seats were tested in the experiment. The practically verified geometry of the closure [16] was adopted to design the dimensions of the gaskets, in particular with respect to the angle α. All the gaskets were designed with the same inner and outer diameters and the same inclination angle α of the working surface. The only difference between the gaskets was in the depth $2h$: two gaskets were designed with $2h$ = 12.5 mm and two others with $2h$ = 25 mm. The outer diameters of the gaskets were made with specific tolerances (Fig. 4) in order to enlarge the limit clearances with respect to the

fit Ø60H7/g6 applied between the holder and the seats. The geometry of the seats is shown in Fig. 5.
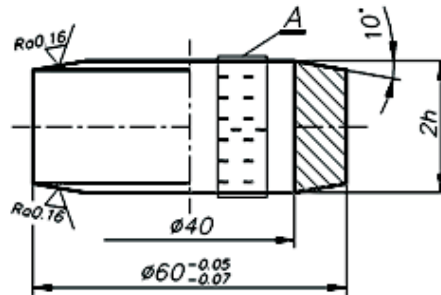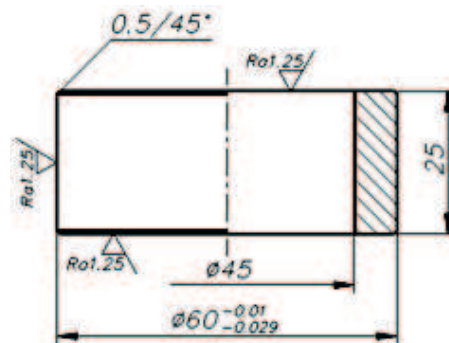

Fig. 4. Geometry of the gasket

Fig. 5. Geometry of the seat

The gaskets and the seats were subjected to the heat treatment in order to obtain appropriate hardness of these elements. Experimentally-verified hardness of the sealing surfaces of the gaskets was of 32÷34 HRC, and the hardness of the seats was of 220÷250 HB.

The aim of the experiment was to determine the circumferential and axial strains along the depth of the gasket with respect to compressive force applied to the closure. The strains were measured with electric resistance wire strain foil gauges. Two strips with 6 gauges were placed at the inner cylindrical surface of each 25 mm gasket: one strip with gauges set in circumferential direction and one strip with gauges set in axial direction. In the case of 12.5 mm gasket, the strips with 3 gauges were applied. Additionally, two single gauges: one circumferential and one axial were located in the central surface of each gasket.

The gauge strips and single gauges for the 25 mm gasket were located and numbered as shown in Fig. 6. The first edge gauges (No. 1 and 2) in the strips were shifted by 2 mm from the face surface of the gasket and the
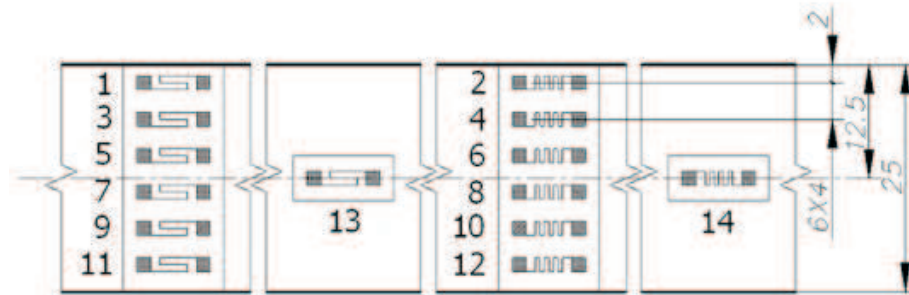
Fig. 6. Detail A in Fig. 4 – localization and numbering of the gauges at the inner surface of
25 mm gasket

distance between the gauges was 4 mm. The axis of the gauge strips and of single gauges were shifted with respect to each other at an angle $\pi/2$. The gauges were connected through a multi-channel switch chests with a static digital resistance bridge, which was driven by a computer recording and processing the data. The test stand prepared for the experiment is shown in Fig. 7 and the gasket with fixed gauges is presented in Fig. 8.

Fig. 7. The test stand prepared for the experiment

Due to the test program, all four sets of gaskets and the corresponding sectional seats were loaded by means of a hydraulic press with the controlled compressive force increasing from 0 to 200 kN. The strains were measured

Fig. 8. The examined gasket with fixed gauges

and recorded at every 25 kN. After unloading and disassembling the closures, the plastic deformation at the contact surface of the seats were measured.

Table 1.

Strength properties of materials applied for the gaskets and the seats

Steel	Source		E [MPa]	$R_{0.05}$ [MPa]	$R_{0.2}$ [MPa]	R_m [MPa]	$\varepsilon_{0.05}$ [%]	$\varepsilon_{0.2}$ [%]	ε_{max} [%]
40H2MF Gasket	Test	mean	2.065×10^5	565.98	705.43	968.00	0.323	0.542	2.412
	PN				1050	1250			9
45HN Seat	Test	mean	2.064×10^5	809.12	812.46	918.50	0.460	0.711	8.802
	PN				850	1050			10

The material tests were carried out to determine the real mechanical properties of materials applied for the gaskets and the seats. Two cylindrical specimens of 5 mm diameter were subjected to the same heat treatment (quenching and tempering) as the corresponding elements, and prepared for the static tensile tests. The obtained strength properties of both steels, calculated as arithmetic means of the two tests, are given in Tab. 1, together with the standard values. It should be noted that different masses and dimensions of the specimens with respect to those of gaskets and seats may be the reason for different heat processes and different final mechanical properties of these elements. Moreover, it appears that the heat treatment caused a significant reduction of all mechanical properties ($R_{0.2}$, R_m, and ε_{max}) of gasket material with respect to the standard data. The appropriate practical relation between the strength properties of the gasket and the seat was changed. Neverthe-

less, lower strength properties of the examined gaskets have no influence on general conclusions resulting from the experiment.

4. Analytical gasket models and solution of the contact region

The results of experiment were compared with the solution for the analytical simplified shell model of the gasket and for the thick-walled model. Several computational models of the closure with "2-delta" gasket were created and investigated in [7] with the aim of selecting the simplest and most effective, but also sufficiently precise one, which could be applied in engineering calculations. The "2-delta" gaskets met in engineering applications are mostly used to seal openings of small diameter, and typically are of large thickness ratio and of small length (depth) $2h$. Analytical shell model of the gasket, adequate to be used for practically applied dimensions, was developed on the basis of the bending shell theory, in which (like for short shells) some terms in the differential equation of deflection could not be neglected [12]. The thick-walled model of the gasket was introduced using modified Lamé solution.

Special attention should be paid to the contact region, because its width is considered to be the critical sealing parameter responsible for the leak tightness of the closure. The relatively high assembly force together with high hardness of the gasket lead to plastic deformation of the seat edges. Under the assumption that the gasket material is perfectly rigid and the seat material is perfectly plastic, and that there is no friction at the contact surface, the problem of plastic deformation may be solved following the well-known problem of truncated wedge subjected to pressure by lubricated flat punch [5, 9]. Additional assumption of plain strain state leads to an analytical solution on the basis of pseudo-steady plastic flow and the shear line pattern [4]. Dislocation of the material and final geometry of the deformed seat are shown in Fig. 9. The pressure q at the contact surface may be determined using Lévy method

$$q = R_{es}(1 + \gamma), \tag{1}$$

where γ is an angle between the shear lines within the triangles AEB and ADC, and R_{es} stands for the yield point of the seat material.

The geometric parameters e and f of the deformed contact region can be readily determined in terms of seat displacement a and of angle α employing the condition that point C must be located at the undeformed, straight-line segment of the seat

$$e = \frac{c\tan\alpha}{\cos\alpha - \sin(\alpha - \gamma)}a, \quad f = \frac{\sin(\alpha - \gamma)}{\tan\alpha\,[\cos\alpha - \sin(\alpha - \gamma)]}a. \tag{2}$$
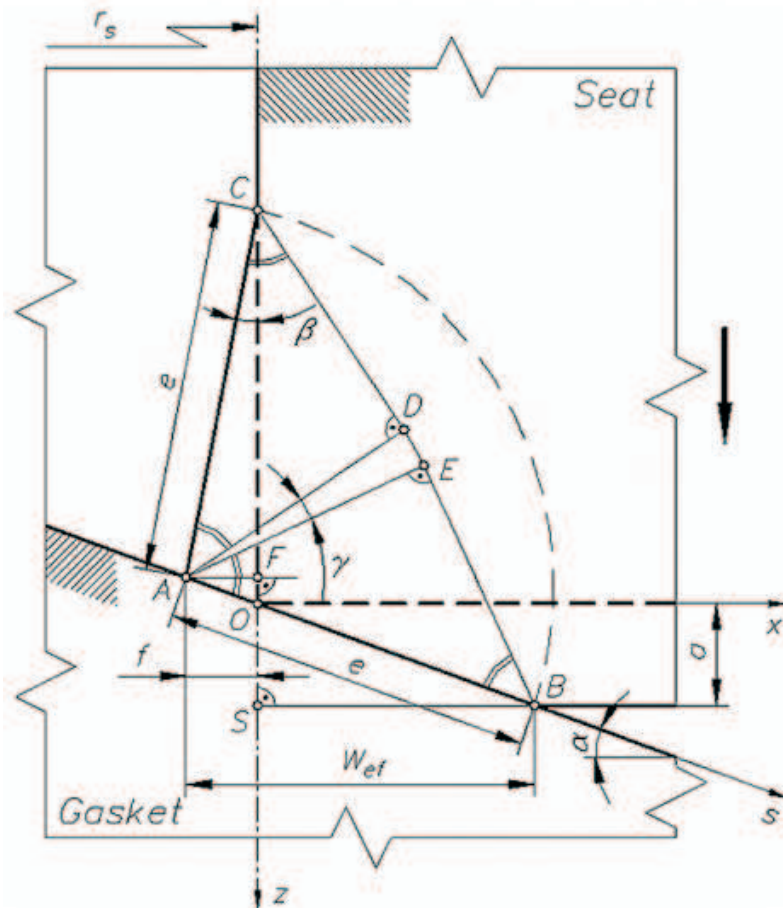
Fig. 9. Dislocation of material and geometry of the deformed seat compressed by a rigid gasket –
part of the contact surface

The assumption of incompressibility of the material (equality of the areas of triangles OSB and OAC) leads, after some simple trigonometric rearrangements, to an implicit equation relating the angles α and γ

$$2 \sin (\alpha - \gamma) [\cos (\alpha - \gamma) + 2 \sin \alpha] - \sin 2\alpha = 0, \tag{3}$$

which needs a numerical procedure to be solved.

The presented solution is of practical meaning only if the width e (or W_{ef}) of the contact region is known in advance. The industrial engineering experience gathered while operating the closures with "2-delta" gaskets is helpful to estimate such a magnitude of the width e which ensures the leak tightness under the working pressure p. The necessary contact pressure q may be then determined from eq. (1), where the angle γ is described by

eq. (3). For the known value of width e, the assembly force F applied to the gasket should be

$$F_{an} = \pi \left(2r_s + e\cos\alpha - 2f\right) \left[eq\cos^2\alpha + \frac{1}{4}\left(2r_s + e\cos\alpha - 2f\right)p\right], \quad (4)$$

where the correction associated with internal operating pressure p is introduced. The seat displacement a and elevation f of point A above OC can be determined from eqs. (2).

It should be mentioned that small value of the inclination angle α of the gasket working surface causes that the angle γ is even more less. For the exemplary "2-delta" gasket in Fig. 1, we have the angle $\alpha = 0.1745$ rad and consequently the angle $\gamma = 0.0465$ rad. For this reason, the contact pressure q calculated from eq. (1) is not too much greater than yield point R_{es} of the seat material.

5. Numerical calculations (FEM)

The high magnitude of assembly force, sharp edge and relatively lower strength properties of the seat lead to plastic deformations in the vicinity of the contact region. Physical nonlinearity of materials must be then taken into account. The problem becomes nonlinear both from the geometrical and physical point of view. The precise solution can be effectively arrived at applying numerical simulation. The numerical calculations were carried out employing FEM method [1, 6, 14]. For that purpose the ANSYS® finite element code was implemented [15].

The gaskets and the seats were made of materials which strength properties were experimentally verified. The character of nominal load-deflection curves suggests multi-linear approximation of $\sigma = \mathrm{f}(\varepsilon)$ relationship shown in Fig. 10. The parameters of approximation were calculated from the set of equations

$$\begin{aligned} \sigma &= E\varepsilon, & \varepsilon &\leq \varepsilon_{0.2}, \\ \sigma &= E_t\varepsilon + R_{0.2} - E_t\varepsilon_{0.2}, & \varepsilon_{0.2} &\leq \varepsilon \leq \varepsilon_{\max}, \end{aligned} \quad (5)$$

where the tangent modulus is $E_t = (R_m - R_{0.2})/(\varepsilon_{\max} - \varepsilon_{0.2})$. Perfectly elastic materials were assumed for the stripper punch and the holder.

The analysis of full 3D structure leads to a big-size and time-consuming numerical task. A significant reduction of the task (to 2D problem) may be obtained under well-based assumption of axial symmetry of the investigated structure subjected to axially distributed loading. The numerical calculations were carried out for the half part of an arbitrary chosen axial cross section of the gasket and the seat. The higher order PLANE82 finite elements were
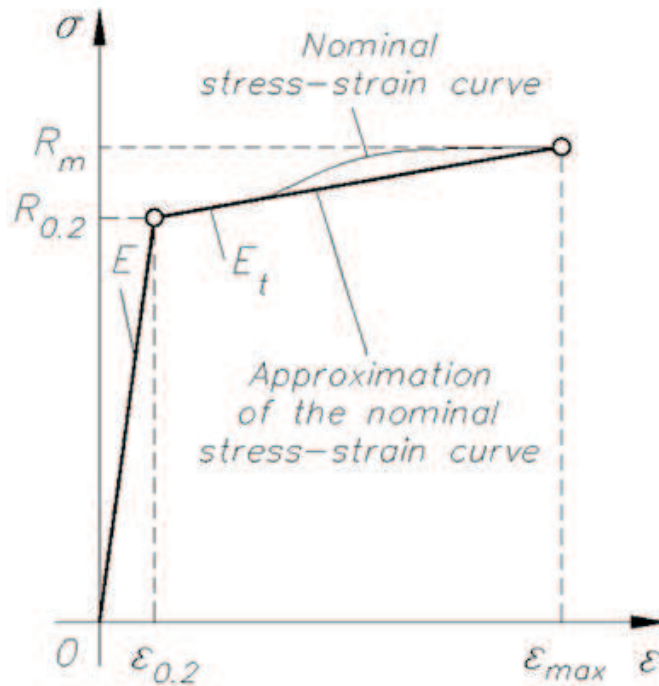
Fig. 10. Approximation of the nominal stress-strain curve of materials (not to scale)
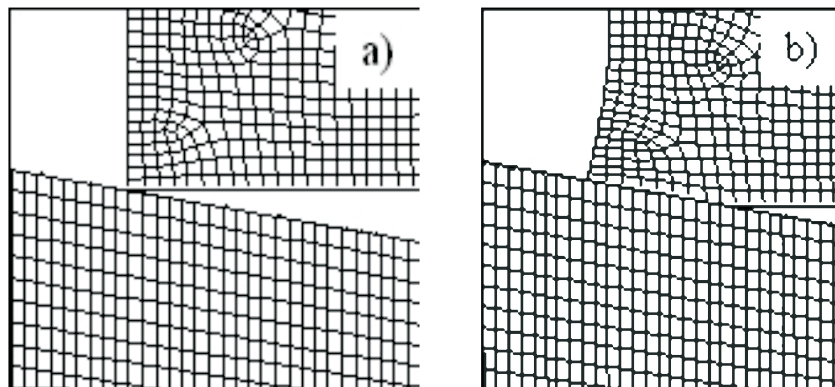

Fig. 11. Exemplary mesh of finite elements in the vicinity of the contact region: a) – initial, b) – after loading

applied to approximate the body of the structure. The shape of the finally-used finite element mesh was determined under the assumption that the mesh must be relatively dense in the vicinity of the contact region, and should remain coarse far from the contact zone, however, a smooth transition of element sizes when moving outside the contact region must be ensured. Exemplary

mesh of finite elements in the vicinity of the contact region is shown in Fig. 11. The density of finite element mesh was controlled according to the error criterion [11].
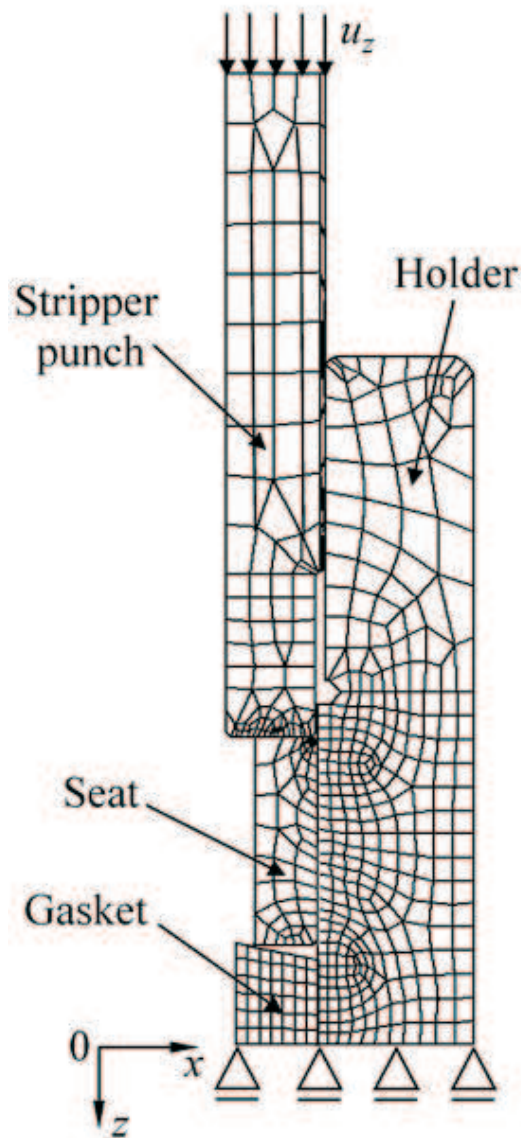

Fig. 12. Distribution of the model into regions, mesh of finite elements and specification of introduced boundary conditions

Local stress concentrations and large strains at the contact surface suggest that the analyzed problem must be considered as a contact one [13]. The

TARGE169 and CONTA172 elements adapted to axial symmetry and plain tasks were used to create the contacting pairs. The higher order elements were applied with mid-side nodes included, which ensured higher accuracy of the solution. The dry (Coulomb) friction at the contact surfaces was introduced into the proposed finite element model.

Specification of the applied boundary conditions is shown in Fig. 12. The displacements of nodes in the central surface of the structure were locked in z axis direction. The kinematic boundary conditions were adopted instead of those caused directly by force F to improve the stability of solution. All nodes of the upper surface of the stripper punch were forced to move at a certain displacement u_z in the z axis direction. The loading was finally determined at the end of iterative procedure applying FSUM functions to the nodes of known displacements. The contact elements at the surface between the stripper punch and the seat were removed. The same boundary conditions were applied to the contacting nodes of both members, although different strength properties of the members were preserved.

6. Verification of applied assumptions

Prior to the analytical and numerical calculations, the true value of friction coefficient μ_1 at the working surface of the closure had to be determined. Compatibility of experimentally measured value of the contact width W with the appropriate value obtained applying FEM method seems to be the most adequate criterion. The results of FEM calculations for the examined closure arrived at for several values of friction coefficient μ_1 are presented in Fig. 13 together with the mean experimental value $W_{mean} = 0.90$ mm. Eventually, the final analytical and numerical calculations were executed applying $\mu_1 = 0.40$ at the contact surface. This value corresponds to that usually met in some cold plastic metals working processes, which are similar, with respect to physical phenomena, to formation of the plastic region in the considered closure. The friction coefficient $\mu_2 = 0.20$ was applied between the outer surface of the gasket and the holder.

The outer diameters of the gaskets and the hole in the holder were made with prescribed dimensional tolerances in order to ensure an appropriate clearance with respect to practical operating recommendations. The corresponding limit radial clearances at the outer surface of the gasket appeared to be: minimum 0.025 mm and maximum 0.050 mm. The maximum radial displacement of the gasket at this surface under the load $F = 200$ kN equals 0.004 mm and is much lower than the minimum clearance. It appears, however, that under the load $F = 150$ kN the gasket came in touch with the holder and the radial displacement of the gasket was blocked. It may be
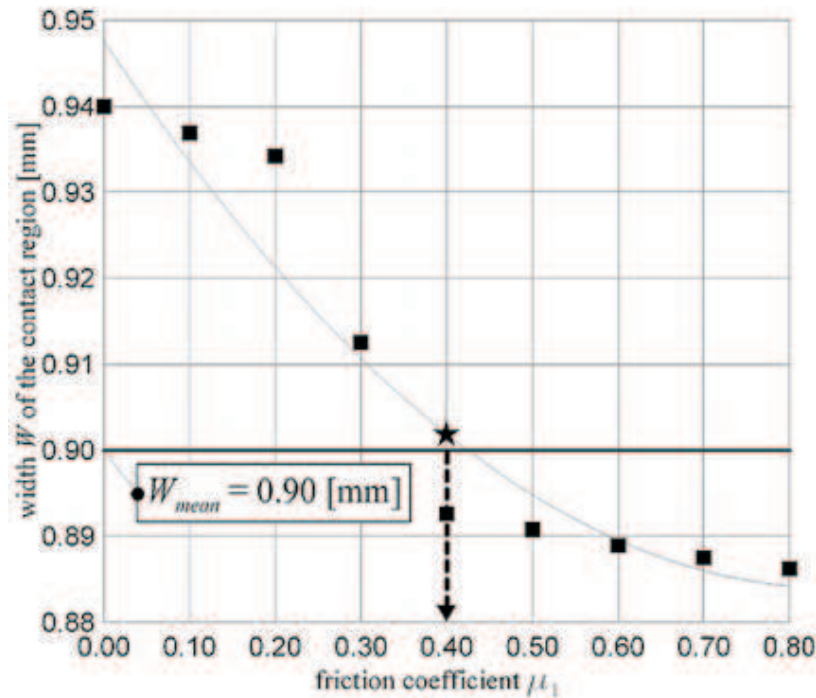
Fig. 13. Width W of the contact region versus friction coefficient μ_1. Bold solid line – mean experimental value, ■ – FEM calculations

seen in Fig. 14, where circumferential σ_ϕ and axial σ_z stresses obtained experimentally at the midpoint of the inner surface of the gasket are plotted versus assembly force F. Such an effect is caused by the assembly axial error of the gaskets with respect to the seats; this notion is confirmed by asymmetry of the plastic deformation of the seats. The appropriate change of boundary conditions was introduced both in the analytical and numerical approach to simulate the observed effect.

The metallographic specimens were prepared to determine the micro-hardness of the gaskets and the seats. The measurement revealed that the heat treatment caused through-hardening of these elements. For this reason, the analytical and numerical calculations were carried out under the assumption that the gaskets and the seats were made of homogeneous material of properties such as those obtained in material tests.

7. Comparison of experimental results with analytical approach and FEM simulation

The experimental results were compared with analytical and numerical calculations for the gaskets of the depth $2h = 25$ mm under the load $F =$
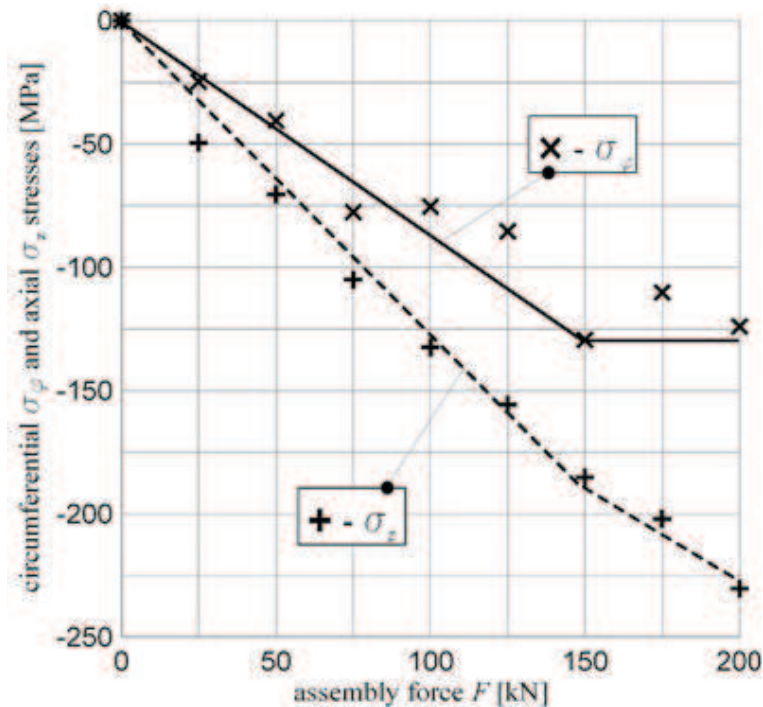
Fig. 14. Circumferential σ_ϕ and axial σ_z stresses at the midpoint of the inner surface of the gasket versus assembly force F

200 kN. The circumferential ε_ϕ and axial ε_z strains at the inner cylindrical surface of the gasket are presented in Figs. 15 and 16 versus z coordinate parallel to the axis of the gasket. The experimental data were calculated as arithmetic means of two tests carried out for gaskets of the same depth. It appears that the strains measured in the tests remain in fairly good agreement with the strains obtained with the FEM calculations (bold solid lines) in the outer parts of the gasket, but in the middle region the difference is rather significant. It should be noted, however, that the strains measured by means of the gauges placed in the vicinity of the gasket edge (No. 1, 2, 11 and 12 in Fig. 6) might be disturbed by the free edge and the significant contact pressure.

The strains calculated with the use of the analytical shell model (fine solid lines) are overestimated with respect both to the test results and to the FEM results. Under assembly conditions ($p = 0$), only the axial strain may be determined for the thick-walled model, while the circumferential strain is zero (dashed lines).

The main reason for performing the stress-strain analysis of structural elements is localization of the critical regions where the stress concentration
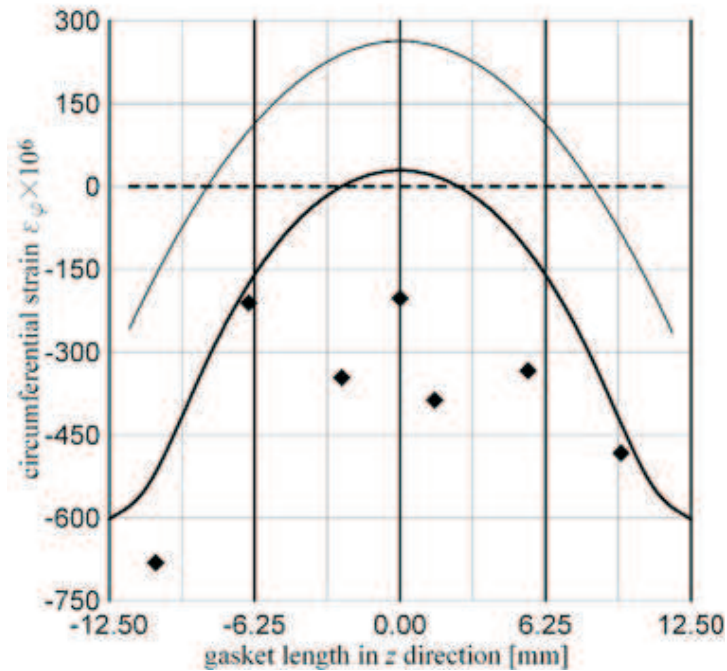
Fig. 15. Circumferential strain ε_ϕ at the inner surface of the gasket versus z coordinate: ◇ – experimental results, bold solid line – FEM results, fine solid line – analytical shell model, dashed line – thick-walled model

appears, and reduction of equivalent stress acting there to the permissible value. The maximum equivalent stress σ_{eq} occurs at the inner surface of the gasket at the mid point $z = 0$. Examination of equivalent stress distributions at this surface, presented in Fig. 17, leads to the conclusion that the maximum value of σ_{eq} obtained with FEM computations (bold solid line) is overestimated with respect to the maximum experimental value by 34%, while the analytical shell model (fine solid line) generates the overestimation by 61%. The equivalent stress determined with the use of thick-walled model (dashed line) is equal to the constant compressive stress in the gasket and is lower by 27% then the maximum experimental value. Additionally, the equivalent stress distributions at the outer surface of the gasket, calculated by means of FEM method and the analytical shell model, are shown in Fig. 17 (bold and fine center lines, respectively). The results for the analytical shell model are overestimated in this case with respect to the FEM results, too. The maximum difference can be observed in the outer part of the gasket.
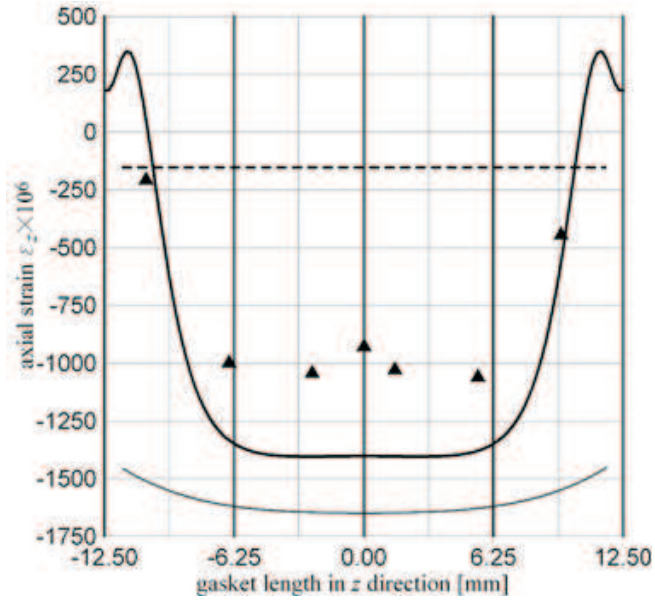
Fig. 16. Axial strain ε_z at the inner surface of the gasket versus z coordinate: ▲ – experimental results, bold solid line – FEM results, fine solid line – analytical shell model, dashed line – thick-walled model
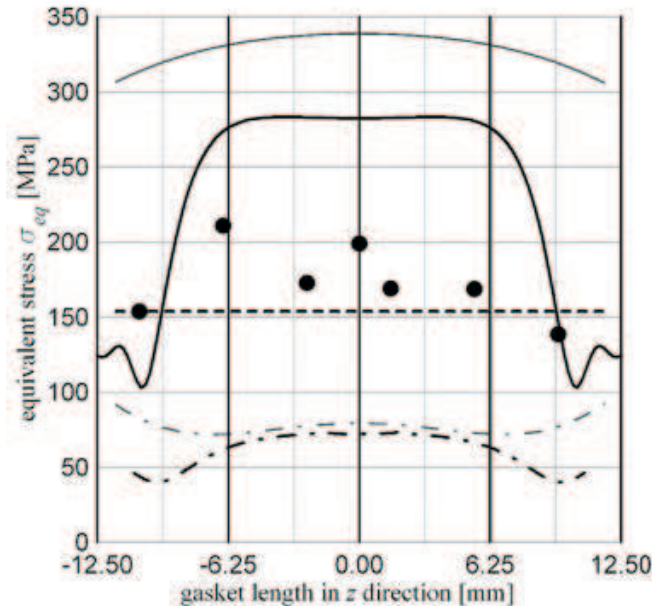

Fig. 17. Equivalent stress σ_{eq} at the inner surface of the gasket versus z coordinate: ? – experimental results, bold solid line – FEM results, fine solid line – analytical shell model, dashed line – thick-walled model
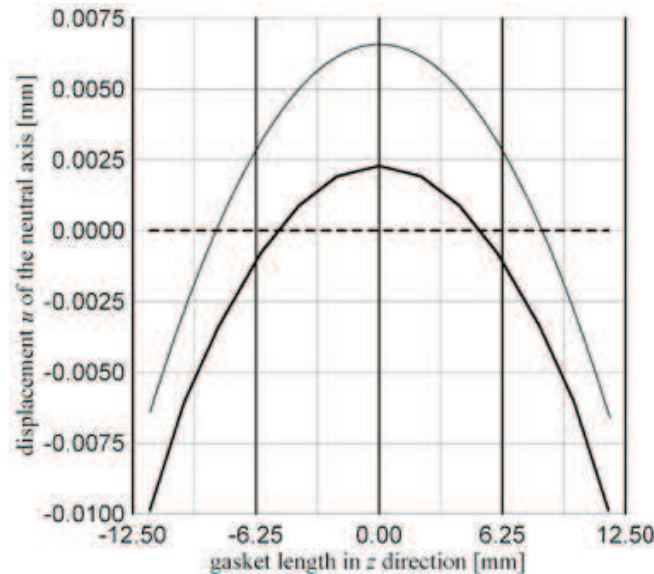
Fig. 18. Displacement u of the neutral surface of the gasket versus z coordinate: bold solid line –
FEM results, fine solid line – analytical shell model, dashed line – thick-walled model

The displacement u of the neutral surface of the gasket versus z coordinate is presented in Fig. 18, where bold solid line corresponds to FEM computations and fine solid line corresponds to the analytical shell model. The displacement of the neutral axis of thick-walled model (dashed line) subjected to the assembly loading equals zero. The distributions of numerical as well as analytical displacement reveal a distinct influence of bending in the axial cross-section, which is caused by an eccentric compressive loading applied to the sealing surfaces of the gasket. The same effect is observed in the experimental strain distributions.

The contact pressure q and the equivalent stress σ_{eq} at the working surface of the gasket computed with the use of FEM simulation are depicted in Fig. 19 versus s coordinate. The s axis is defined in Fig. 9 and its origin is identical with the inner edge of the gasket. The distribution of contact pressure (bold line) is in agreement with the prediction, decreasing along the contact width e from the maximum value at the beginning. The maximum value of $q = 1641$ MPa appears at the point $s = 2.4475$ mm, then the contact pressure decreases to $q = R_{es} = 812$ MPa at the point $s = 3.3205$ mm and reaches zero at the point $s = 3.3540$ mm. The total width of contact region is $e = 0.9064$ mm ($W = 0.8926$ mm) while the contact pressure q is greater than the yield point $R_{0.2}$ of the seat material at the width $e_{ef} = 0.8730$ mm ($W_{ef} = 0.8597$ mm). The analytical value of contact pressure – eq. (1)
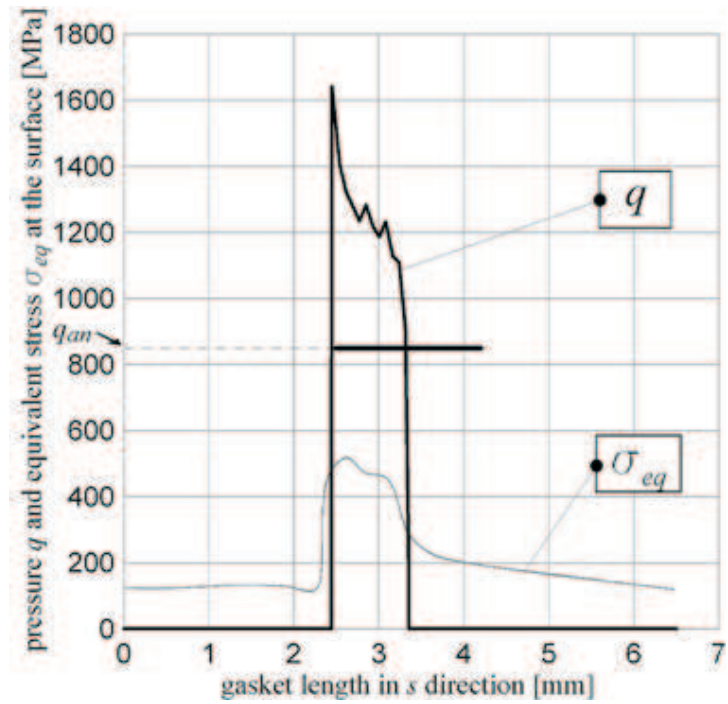
Fig. 19. Contact pressure q and equivalent stress σ_{eq} at the sealing surface of the gasket under
assembly force $F = 200$ kN ($p = 0$) versus s coordinate
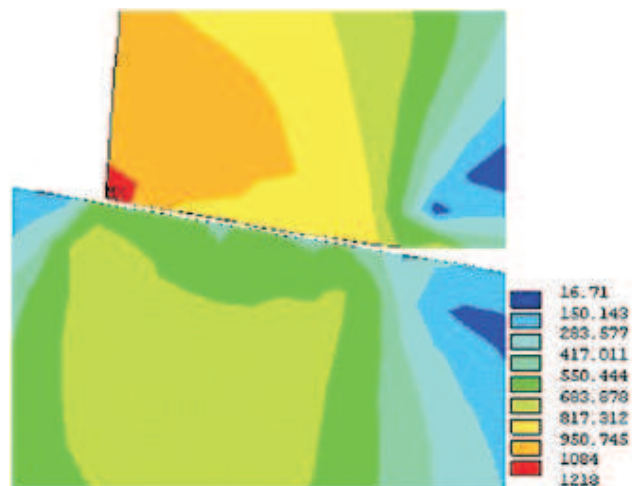

Fig. 20. Distribution of equivalent stress σ_{eq} in the vicinity of the contact region under assembly
force $F = 200$ kN ($p = 0$)

q_{an} = 850 MPa presented Fig. 19 is only a bit greater than the yield point R_{es} of the seat material. The results of numerical calculations of the equivalent stress σ_{eq} in the contact region are shown in Fig. 20, and are additionally depicted in the contact surface of the gasket in Fig. 19 (fine line).
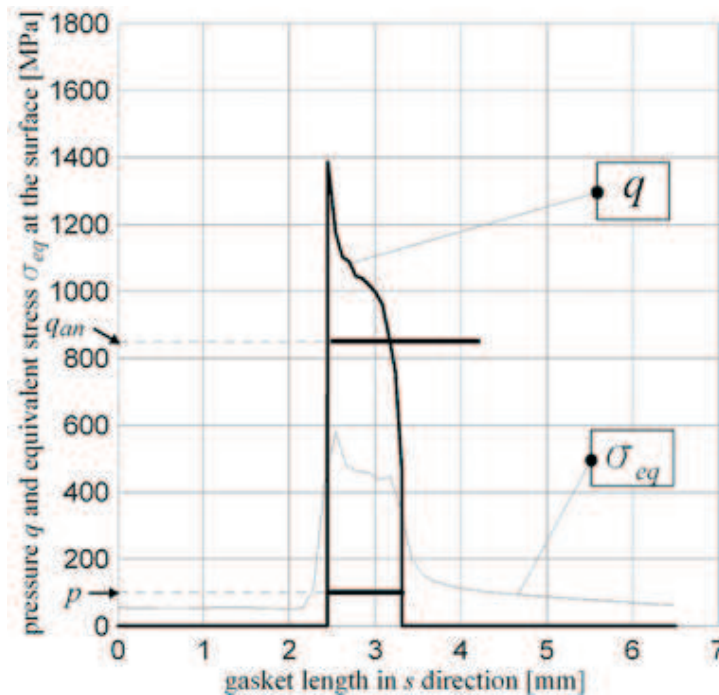

Fig. 21. Contact pressure q and equivalent stress σ_{eq} at the sealing surface of the gasket under the force $F^* = 75.3$ kN and operating pressure $p = 100$ MPa versus s coordinate

The presented distribution of the contact pressure q at the sealing surface of the closure members is obtained under the assembly conditions. The operating pressure p applied to the closure changes the distribution. The changed distribution of contact pressure is shown in Fig. 21 for an arbitrarily chosen operating pressure $p = 100$ MPa. The assembly force decreases strongly, dropping to $F^* = 74.3$ kN (at 63%), and so happens with the maximum value of contact pressure q (to 1387 MPa at 15%) and the corresponding total width of the contact region which is necessary to seal the closure (to $e = 0.8661$ mm at 4%). Under the assumption that leak tightness of the closure is ensured where the contact pressure q exceeds the operating pressure p, the effective seal is obtained at the width $e_{ef} = 0.8663$ mm ($W_{ef} = 0.8531$ mm). The maximum value of the equivalent stress σ_{eq} in the gasket increases from 518 MPa (Fig. 20) to 579 MPa (Fig. 22). A detailed numerical analysis of
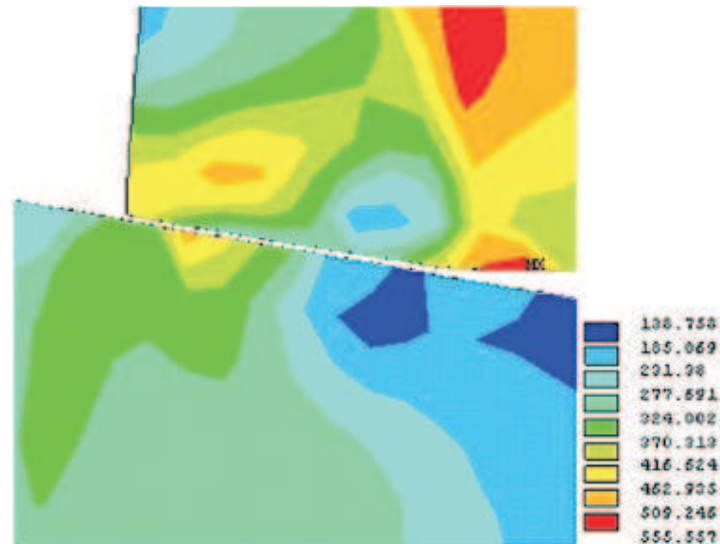
Fig. 22. Distribution of equivalent stress σ_{red} in the vicinity of the contact region under the force
$F^* = 75.3$ kN and operating pressure $p = 100$ MPa

the leak tightness of the closure with metal "2-delta" gasket with respect to
the operating pressure is presented in [8].

The marks of plastic deformation of the seats revealed axial eccentricity
(Fig. 23), so it was evident that both segments of the seat were not set up
in axially-aligned position with the gasket during the experiment. For this
reason, the width W and elevation f (in the plane normal to the gasket axis)
were measured in eight cross-sections shifted at an angle of $\pi/4$. The mea-
surement was carried out by means of the coordinate device. The coordinates
of points were gathered and recorded using a scanning probing head. The
distributions of W and f versus the perimeter of a certain seat, denoted as
No. 5, is shown in Fig. 24. The values of W and f were calculated for each
seat applying minimum chi-square method and are collected in Tab. 2 as
arithmetic means for eight investigated seats.

The test results are compared with analytical solution of the contact
region and FEM calculations in Tab. 2. The displacement a of the seat was
not measured, but the analytical result is much greater than the numerical
one. The elevation f obtained numerically coincides with the appropriate test
result, however, the analytical approach leads to a value twice greater then
the experimental one.

The width W is the crucial parameter of the closure as it directly de-
termines proper conditions of the leak tightness. The result obtained using
the analytical model is overestimated by 86 % with respect to test result,
while the numerical result (after unloading) is underestimated only by 1 %,
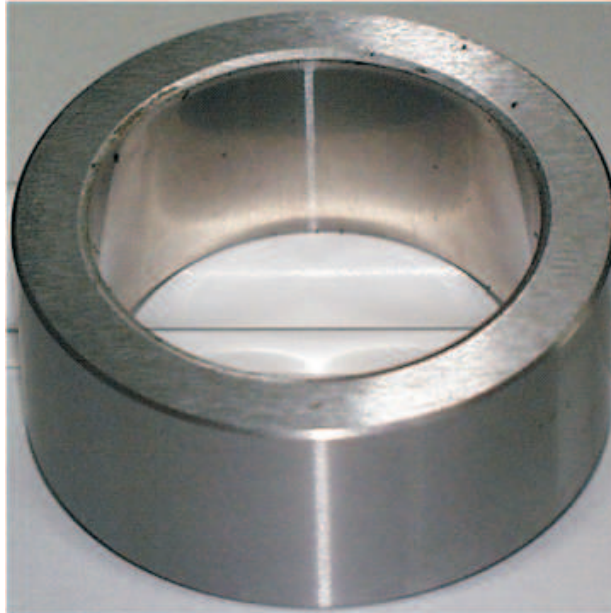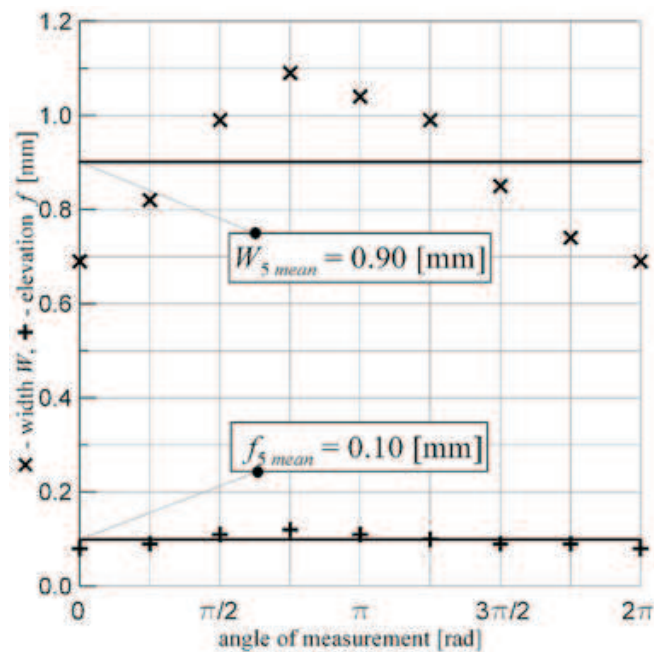
Fig. 23. Mark of plastic deformation of the seat

Fig. 24. Distributions of width W and elevation f versus the perimeter of the seat No. 5

which results directly from the criterion applied to determine the friction coefficient μ_1. A large discrepancy between the analytical solution and the

Table 2.

Comparison of experimental results with analytical solution of the contact region and FEM calculations

		a [mm]	f_{mean} [mm]	W_{mean} [mm]
Test		–	0.09	0.90
Analytical solution		0.2525	0.2133	1.6704
FEM	$F = 200$ kN, $p = 0$ (loading)	0.1580	0.1017	0.8926
	$F^* = 74.3$ kN, $p = 100$ MPa	0.1489	0.0886	0.8529
	$F = 0$, $p = 0$ (unloading)	0.1136	0.0907	0.8923

test or FEM results may be explained by the fact that different approximations of the stress-strain curve of the seat material were applied in the two models. Moreover, the analytical model of the contact region was created under a strong assumption of friction absence. The values of a, f and W depend, in the analytical solution, on the geometry of the closure only, contrary to those found in numerical computations and in the real structure, where the operating pressure p causes their decrease.

8. Final remarks

High-pressure closures with metal "2-delta" gasket are often used in the heavy-duty equipment. However, in opposite to other types of joints (e.g. flanged joints), "2-delta" gaskets are not adequately presented in technical literature. Moreover, their design procedures are not regulated by the code or standards.

It is difficult to carry out an immediate complete numerical analysis of all "2-delta" gaskets while a design project of high-pressure installation contains a large number of closures. Analytical computational models proposed in [7] may be convenient to proceed an initial analysis. A large number of simple calculations can be carry out for different geometry of the closure, different material properties and assembly requirements. The appropriate parameters of the closure may be then determined and applied finally in the detailed FEM verification.

Because of the specific design features of the closure, the appropriate strength of its members may be easily ensured. The analytical shell model leads to results overestimated with respect to FEM calculations, and may be applied to the stress-strain analysis of the gasket as it ensures additionally a certain margin of safety. The analytical and numerical calculations reveal that maximum equivalent stress appears at the mid point of inner surface of the gasket. The same conclusion may be drawn from the distri-

butions of the experimentally measured strains which are not disturbed in this region by the free edge and local stresses concentration at the contact surface.

The basic difficulty in the design of closures with "2-delta" gaskets is to ensure the leak tightness produced by the appropriate assembly force. The magnitude of applied assembly force must be adequate to the material properties and geometry of the mating members, as well as to the operating pressure. The assembly force should produce a specific contact pressure at the contact face of relevant width.

The sealing contact region was analytically solved in the paper with respect to the plastic deformation of the seat. It should be noted, however, that analytical solution leads to the value of contact width nearly twice as large as the experimental or numerical one. This discrepancy must be taken into account in the initial calculations of the leak tightness. The contact pressure q at the working surface of the gasket which is necessary to produce the seal may be analytically determined for the assembly conditions only. The contact pressure exceeds the yield point of the seat material, which coincides with practical approach applied in operating "2-delta" gaskets. The results of numerical calculations lead to the conclusion that operating pressure additionally applied to the closure causes a significant decrease of the contact pressure and related decrease of the width of the contact region. Application of an exemplary operating pressure $p = 100$ MPa produces, in the considered closure, a decrease by 15% and by 4%, respectively. The distribution of the contact pressure is irregular, so an effective seal is obtained at even smaller width. The contact pressure exceeds the applied operating pressure at the width $W_{ef} = 0.8531$ mm with maximum value closer to the inner space of the joint, which makes penetration of the medium more difficult, and prevents loosening of the seal.

Experimental investigations of the closures with "2-delta" gaskets lead to the conclusion that one must warrant high assembly precision with respect to axis alignment. The maximum radial clearance 0.05 mm in the considered closure is eliminated by an axial deviation of $0.27°$. The influence of such an error on the strength of the gasket is negligible, but it worsens the crucial sealing parameters. When there is a reduction in the radial clearance at the outer surface of the gasket, there is also a decrease in the effects of the self-sealing process with respect to the contact pressure q. Moreover, the lost of leak tightness may occur as the asymmetry of the contact region appears. For example, in the present design, the minimum width of the contact region is by 20% lower than its average value.

REFERENCES

[1] Bathe K. J.: Finite element procedures in engineering analysis. Englewood Cliffs, New Jersey, Prentice-Hall, Inc., 1982.

[2] Deininger J., Strohmeier K.: Metalldichtungen für hohe Drücke. Dichtungstechnik, 2000, Heft 1, Mai 2000, pp. 31-35 (in German).

[3] Freeman A. R.: Gaskets for high-pressure vessels. Pressure Vessel and Piping Design. Collected Papers 1927 – 1959. ASME, 1960, pp. 165-168.

[4] Hill R.: The plastic yielding of notched bars under tension. Q. J. Mech. Appl. Math., Vol. 2, 1949.

[5] Hill R., Lee E. H., and Tupper S. J.: The theory of wedge indentation of ductile materials. Proc. Roy. Soc., London (A) 188, 1947, pp. 273-289.

[6] Hughes T. J. R.: The finite element method. Linear static and dynamic finite element analysis. Englewood Cliffs, New Jersey, Prentice-Hall, Inc., 1987.

[7] Krasiński M., Trojnacki A.: Computational model of metal high-pressure "2-delta" gasket. Czasopismo Techniczne, 2009, z. 3-M/2009, pp. 31-58 (in Polish).

[8] Krasiński M., Trojnacki A.: Numerical analysis of leak tightness of metal high-pressure "2-delta" gasket. Acta Mechanica et Automatica, 2009, Vol. 3, No. 1(7), pp. 71-77 (in Polish).

[9] Prager W., Hodge P. G., Jr.: Theory of perfectly plastic solids. N. York, J. Wiley & Sons, Inc., 1951.

[10] Ryś J., Zieliński A.: Sealing of high-pressure vessels by means of double-cone sleeve. Przegląd Mechaniczny, 1977, Vol. 7/77, pp. 224-229 (in Polish).

[11] Stein E.: Error–controlled adaptive finite elements in solid mechanics. West Sussex, JOHN WILEY&SONS, LTD, 2003.

[12] Timoshenko S. P., Woinowsky-Krieger S.: Theory of plates and shells. New York, McGraw-Hill, 1959.

[13] Wriggers P.: Computational contact mechanics. West Sussex, JOHN WILEY&SONS, LTD, 2002.

[14] Zienkiewicz O. C., Taylor R. L.: The finite element method. Vol. 1 The basis, Vol. 2 Solid mechanics. Woburn, Butterworth-Heinemann, 2000.

[15] ANSYS. Release 8.0. Swanson, Analysis System Inc., 2003.

[16] Report TPP–5 Cracow University of Technology: Project of reactor 41/42 V-7 in propylene installation. Kraków, 2000 (in Polish).

Badania doświadczalne metalowej wysokociśnieniowej uszczelki typu „2-delta"

S t r e s z c z e n i e

W pracy przedstawiono wyniki badań doświadczalnych metalowych wysokociśnieniowych uszczelek typu „2-delta" o różnej grubości. Badania przeprowadzono w warunkach montażowych pod obciążeniem montażową siłą ściskającą, bez obciążenia połączeń ciśnieniem roboczym. Na wewnętrznej, cylindrycznej powierzchni uszczelek mierzono odkształcenia obwodowe i osiowe przy

użyciu elektrycznych tensometrów oporowych. Po odciążeniu zmierzono szerokość strefy kontaktu plastycznie odkształconych gniazd. Zostały również wykonane badania materiałowe uszczelek oraz gniazd w celu określenia ich rzeczywistych własności wytrzymałościowych. Wyniki pomiarów porównano z obliczeniami analitycznymi, otrzymanymi w oparciu o uproszczony powłokowy model uszczelki i model grubościenny. W analitycznym opisie strefy kontaktu uszczelki z gniazdem zostały wzięte pod uwagę plastyczne odkształcenia gniazda. Dodatkowo została wykonana numeryczna weryfikacja pomiarów i obliczeń analitycznych za pomocą obliczeń MES, w których uwzględniono nieliniowe własności materiałów połączenia oraz tarcie na powierzchni kontaktu.